Functional Proton Electron Double Resonance Imaging: Concept and Experiment

V. V. Khramtsov[1], K. Shet[1], E. Kesselring[1], S. Petryakov[1], Z. Sun[1], J. L. Zweier[1], and A. Samouilov[1]

[1]Dorothy M. Davis Heart & Lung Research Institute, The Ohio State University, Columbus, OH, United States

NMR imaging, MRI, is used for numerous biomedical and clinical applications but availability of functional imaging is still limited. On the other side, EPR of exogenous paramagnetic probes has unique advantage in functional specificity due to the absence of overlap with endogenous EPR signals. However EPR-based techniques are far from attaining their maximum potential due to technical limitations of EPR and EPR imaging (EPRI). The most successful continuous wave (CW) EPRI technique is based on spectra measurement at numerous magnetic field gradients which requires a long acquisition time, which is often unpractical for biological use. It is further compromised by the limited stability of existing probes. In this work we proposed new modalities of functional imaging in living tissues. To improve spatial and temporal resolution of EPRI we used a proton electron double resonance imaging (PEDRI) approach in combination with a new concept of Variable Field (VF) PEDRI. This allows for functional mapping using specifically designed paramagnetic probes (e.g. oxygen or pH mapping) within MRI high quality spatial resolution and short acquisition time.

Normally PEDRI is acquired at fixed EPR field B_o^E resulting in loss of EPR spectral information. However, dynamic nuclear polarization (DNP) allows for obtaining EPR spectrum from NMR signal detection. A plot of the NMR signal amplitude verses evolution EPR field, B_o^E, provides information similar to a conventional EPR spectrum as shown in Fig.1b for the aqueous solution of the pH-sensitive ATI probe (see Fig.1a for the structure). The DNP spectra of the ATI solutions measured at different pH values demonstrate clear difference in the positions of low- and high-field spectral components due to the difference in the hyperfine splitting constant, Δa_N=0.8 G, between the protonated and deprotonated ATI radicals. The a_N value measured from DNP spectra of ATI probe shows typical pH dependence described by Henderson-Hasselbalch equation and can be used as pH marker in biological systems. However, while DNP spectra measurement provides functional information on the medium (e.g., pH) it does not provide spatial resolution. Moreover, it requires long-time acquisition due to detection of NMR signals after RF irradiation at numerous stepwise changed EPR fields. PEDRI with variable field EPR pre-excitation will allow EPR spectroscopic information to be obtained along with the spatial information on the structure of the object and the distribution of the radical within the object, from the value of the enhancements observed at each pixel. The information obtained is equivalent to that of a 3D or 4D spectral-spatial EPR image along with a superimposed proton MRI. Note that direct spectral-spatial EPRI techniques require long times (typically > 1hr for 4D acquisition), high gradients (≥30 G/cm), and only provide low resolution spatial images.

We hypothesized that valuable spectral parameters at each pixel can be extracted from a limited number of selected PEDRI acquisitions (as little as two) with acquisition time less than a minute. To prove the concept we used the phantom with four capillary tubes filled with solutions of pH sensitive ATI probe prepared at different pH (Fig. 1c). The VF PEDRI acquisitions were performed only at two pre-selected EPR excitation fields which coincide with DNP high-field spectral peak positions of RH^+ and R forms of the probe (Fig. 1b). The two images shown in Figure 1c were acquired in 8.8 s providing field of view (FOV), 30 mm× 30 mm, with resolution 64x64. The ratio of NMR signals at each pixel of these two images is pH dependent and was converted to pH map shown in Fig. 1d. The studies performed with phantom show that a pH resolution of ~0.1 pH units and a spatial resolution of 0.5 mm can be achieved at low NMR field of ~200 G. The data show at least 10 fold decrease in acquisition time for VF PEDRI compared with EPRI for the same phantom and similar spatial and functional resolutions. This is particularly important for *in vivo* applications where the experimental window and stability of the nitroxides are limited. Another advantage of VF PEDRI is slice selectivity of the functional image which is unavailable in CW EPRI. Therefore, VF PEDRI possesses the capacity for functional and anatomical resolution in one experimental set-up (otherwise available only in EPR/NMR co-imaging).

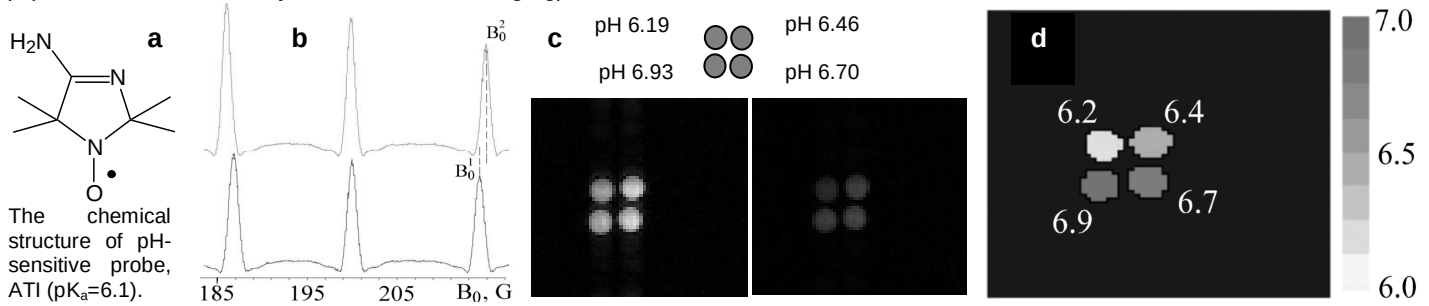

The chemical structure of pH-sensitive probe, ATI (pK_a=6.1).

Fig. 1. (a) Chemical structure of ATI probe and **(b)** FC-DNP spectra of 0.5 mM ATI prepared in 10 mM phosphate–citrate buffer, 28 ml sample volume, at pH 7 (top, R form) and pH 2 (bottom, RH^+ form). Dotted lines are extended from high-field peaks of the spectra to aid the eye. Note that the values of pre-excitation EPR fields corresponding to DNP spectral peaks of RH^+ (B_0^1) and R (B_0^2) forms are shifted by about 0.8 G from each other. The ratio $[RH^+]/[R]$ varies with pH change and at low EPR frequency, when resonances are unresolved, spectral alterations result in the apparent shift in the positions of low- and high-field peaks. **(c)** pH phantom and its PEDRI images acquired at the EPR frequency 567 MHz, and two EPR fields, B_0^1=214.16 G and B_0^2=214.88 G corresponding to peak amplitudes of DNP spectra of the RH^+ and R forms of the probe. Number of excitations, N_{ex}=4 (acquisition time, 4.4 s). **(d)** pH map of phantom calculated from two PEDRI images acquired at different pre-selected EPR excitation fields. Averaged values of pH are given near corresponding capillary tube.

Note that while concept of functional VF PEDRI was demonstrated using the pH probe, it can be also applied for mapping redox state, concentrations of oxygen or glutathione and other biologically relevant parameters of the medium using specifically designed probes. *Supported by grants NIH KO1 EB03519, R01 EB004900, and EB00890.*